A NOVEL, FULLY COUPLED FLOW AND GEOMECHANICS MODEL IN POROUS AND FRACTURED GEOTHERMAL RESERVOIRS

Litang Hu[a,b*], Philip H. Winterfeld[b], Perapon Fakcharoenphol[b], Yu-Shu Wu[b], Keni Zhang[c,a], and Tianfu Xu[c,d]

[a] College of Water Sciences, Beijing Normal University, Beijing 100875, PR China
[b] Petroleum Engineering Department, Colorado School of Mines, Golden, CO, USA, 80401
[c] Earth Sciences Division, Lawrence Berkeley National Laboratory, Berkeley, California, 94720, U.S.A
[d] College of Environment and Resources, Jilin University, Changchun, Jilin 130026, PR China
e-mail: litanghu@bnu.edu.cn

ABSTRACT

Numerical simulation of thermal-hydrologic-mechanical (THM) processes in porous and fractured media has become increasingly important and valuable for its role in the understanding of fluid flow, heat transfer, and rock deformation in stress-sensitive geothermal reservoirs. This paper presents a novel, fully coupled fluid-flow and geomechanics simulator (TOUGH2-EGS), in which the fluid flow portion is based on the general-purpose numerical model TOUGH2/EOS3, and the geomechanical portion is developed from the linear elastic theory for a thermo-poro-elastic system using the Navier equation. The multiple interacting continua method is applied to simulate flow in the fracture and fracture-matrix interaction. Porosity and permeability depend on effective stress, and several correlations describing that dependence are incorporated into the simulator. The established model is verified against analytical solutions for the one-dimensional dual-porosity consolidation problem by Wilsion and Aifantis (1982). Two cases—a five-spot injection and production pattern, and the Rutqvist and Tsang (2002) model—are examined for analyzing the effects of changes in pressure on fracture flow and rock deformation. The results demonstrate that our new model can be used for field-scale geothermal reservoir simulation of fluid flow and geomechanical effects in porous and fractured media.

INTRODUCTION

Geomechanical effects within porous and fractured media must be seriously considered with respect to enhanced geothermal systems, particularly in analyzing associated formation subsidence and stress-sensitive fractured reservoirs (Merle et al., 1976; Lewis and Schrefler, 1998; Settari and Walters, 2001; Boutt et al., 2011). Moreover, the coupling of geomechanics with porous-media fluid and heat flow would also be valuable for a variety of other technical problems—e.g., soil shrinkage from water evaporation and soil heaving due to water freezing; formation permeability and porosity changes; rock deformation associated with heavy oil recovery processes such as steam assisted gravity drainage (SAGD) or from cold water injection and steam/hot water production in geothermal fields. Furthermore, most geothermal reservoirs are situated in igneous and metamorphic rocks that have low matrix permeability. Well-connected cracks and fractures provide highly permeable fluid-flow paths through unfractured tight rock matrix. Artificial fractures or hydraulic fractures will be vital in providing additional highly permeable flow paths for underground fluid flow and heat exchange. For all these issues, numerical simulation of thermal-hydrologic-mechanical (THM) processes in porous and fractured media has become increasingly important.

Winterfeld and Wu (2011) have recently presented a fully coupled THM model based on a generalized version of Hooke's law in porous media, and have verified the model using several sample problems. However, how to simulate geomechanical behavior in fractured media remains a question. The first conceptualization of model flow in fractured media is the double-porosity concept, originally developed by Barenblatt et al. (1960), and later developed to classical double-porosity concept for modeling flow in fractured, porous media developed by Warren and Root (1963). The multiple interacting

continua (MINC) numerical approach has been used to simulate fracture and porous-matrix flow and interactions (Pruess and Narasimhan, 1985). The basic concept of MINC is that changes in fluid pressures (due to the presence of recharge or discharge from boundaries of the model domain) will propagate rapidly through the fracture system, while only slowly invading tight matrix blocks. Therefore, changes in matrix conditions will be controlled locally by the distance from the fractures. Fluid flow from the fractures into the matrix blocks or from the matrix blocks into the fractures can then be modeled by means of one-dimensional strings of nested gridblocks (Pruess et al., 1999). Doughty et al. (1999), in thoroughly examining and comparing fractured rock modeling methods for flow and transport processes in the unsaturated zone (UZ) at Yucca Mountain, NV, found that the MINC approach with multi-matrix-gridblocks gives the most accurate infiltration pulse and tracer arrival time among all methods. Wu et al. (2004) introduced the triple continuum concept, consisting of (1) tight rock matrix, (2) small-scale fractures, and (3) large-scale fractures. Each continuum can interact with any other, and global flow takes place in large fractures and rock matrix continua.

This paper will present a novel, fully coupled fluid flow and geomechanical simulator (TOUGH2-EGS) in detail, and then the model will be verified, through a 1D flow-geomechanical case using the dual porosity method for fractured reservoirs, by comparison with analytical solutions. Finally, two cases, one involving a five-spot injection and production pattern, and the other the Rutqvist and Tsang (2002) model, are simulated for analyzing how changes in pressure affect fracture flow and rock deformation.

MATHEMATICAL MODEL

Formulation of fluid and heat flow in porous and fractured media

Our new simulator was developed based on the general framework of mathematical and numerical models, which solve mass- and energy-balance equations describing fluid and heat flow in general multiphase, multicomponent systems (TOUGH2/EOS3). Fluid flow is described using a multiphase extension of Darcy's law. Heat flow is governed by conduction and convection, including sensible as well as latent heat effects. Following Pruess et al. (1999), the mass- and heat-balance equations in each model subdomain or REV of an EGS can be written as in Table 1. The MINC method is used to simulate fracture-fracture flow or fracture-matrix flow.

Table 1. Equations of fluid and heat flow solved in TOUGH2-EGS

Description	Equation
Conservation of mass and energy	$\frac{d}{dt}\int_{V_n} M^\kappa \, dV_n = \int_{\Gamma_n} \mathbf{F}^\kappa \bullet n \, d\Gamma_n + \int_{V_n} q^\kappa \, dV_n$ $\kappa = 1, 2, 3$
Mass accumulation	$M^\kappa = \phi \sum_{\beta w} S_{\beta w} \rho_{\beta w} X^\kappa_{\beta w}$, $\kappa = 1, 2$
Mass flux	$\mathbf{F}^\kappa = \sum_{\beta w} X^\kappa_{\beta w} \rho_{\beta w} \mathbf{u}_{\beta w}$, $\kappa = 1, 2$
Energy flux	$\mathbf{F}^3 = -\lambda_T \nabla T + \sum_{\beta w} h_{\beta w} \rho_{\beta w} \mathbf{u}_{\beta w}$
Energy accumulation	$M^3 = (1-\phi)\rho_R C_R T + \phi \sum_{\beta w} \rho_{\beta w} S_{\beta w} U_{\beta w}$
Phase velocity	$\mathbf{u}_\beta = -k \frac{k_{r\beta w}\rho_{\beta w}}{\mu_{\beta w}} (\nabla P_{\beta w} - \rho_{\beta w} \mathbf{g})$

Formulation of geomechanics in porous and fractured reservoir

The poroelastic version of the Navier equations for matrix (Jaeger et al., 2007) is as Equation 1. The definition of symbols is shown in the Symbol Chapter.

$$G\nabla^2 \bar{u} + (G+\lambda)\nabla(\nabla \cdot \bar{u}) = -\bar{F} - \alpha \nabla P - 3\beta K \nabla T \quad (1)$$

The poroelastic version of the Navier equations for matrix and fractures (Bai and Roegiers, 1994) is

$$G\nabla^2 \bar{u} + (G+\lambda)\nabla(\nabla \cdot \bar{u}) = -\bar{F} - \alpha_f \nabla P_f - \alpha_m \nabla P_m - 3\beta_m K_m \nabla T_m - 3\beta_f K_f \nabla T_f \quad (2)$$

where

$$a_f = 1 - K_f / K_m; \;\; a_m = K_f / K_m (1 - K_m / K_s) \quad (3)$$

Here, K_f is the fracture medium bulk modulus, K_m is the bulk modulus of the matrix, and K_s is the solid bulk modulus.

Strain can be expressed in terms of a displacement vector, u. The displacement vector points from the new position of a volume element to its previous position. The strain tensor is related to the displacement vector by

$$\bar{\bar{\varepsilon}} = \frac{1}{2}[\nabla \bar{u} + (\nabla \bar{u})^T] \quad (4)$$

Hook's law for the normal stress of a thermoporoelastic dual-permeability medium, generalized from Bai et al., 1995, is

$$\tau_{ll} - (\alpha_f p_f + \alpha_m p_m + 3\beta_f (T_f - T_{ref}) + 3\beta_m (T_m - T_{ref})) = 2G\varepsilon_{ll} + \lambda(\varepsilon_{xx} + \varepsilon_{yy} + \varepsilon_{zz}), l = x, y, z \quad (5)$$

The volumetric strain is obtained from summing the normal stress components in the above equation:

$$K\varepsilon_v = \tau_m - (\alpha_f p_f + \alpha_m p_m + 3\beta_f (T_f - T_{ref}) + 3\beta_m (T_m - T_{ref})) \quad (6)$$

The above two equations can be generalized to the MINC formulation by replacing the fracture (f) and matrix (m) terms with a summation over MINC, for example:

$$K\varepsilon_v = \tau_m - \sum_{i=1}^{N} (\alpha_i p_i + 3\beta_i (T_i - T_{ref})) \quad (7)$$

For each set of MINC blocks, there is one mean stress and one volumetric strain. Mean stress is a gridblock primary variable. The mean stress equation of discretation is

$$\frac{3(1-\nu)}{(1+\nu)} \nabla^2 \tau_m = -\nabla \cdot \bar{F} + \frac{2(1-2\nu)}{(1+\nu)} \sum_{i=1}^{N} (\alpha_i \nabla^2 P_i + 3K\beta_i \nabla^2 T_i) \quad (8)$$

Rock property corrections

When the spatial average stress distribution is calculated, permeability and porosity are both dependent on effective stress:

$$k = k(\sigma') \quad (9)$$

$$\phi = \phi(\sigma') \quad (10)$$

These relationships are based on experimental formula and can be input to the model. Since bulk volume is related to porosity, we also allow bulk volume to depend on effective stress and pore pressure

$$V_b = V_b(\sigma', P) \quad (11)$$

Code integration

The mean total stress is added as an additional primary variable. Thus there are four primary variables: pressure, temperature, air mass fraction, and the mean total stress. Secondary variables such as liquid saturation and volumetric strain are calculated from the primary variables. Pressure, temperature, and mean total stress initialization parameters are first input into the model, and the initial stress field is then calculated from them. Finally, pressure, temperature, air mass fraction, and mean total stress are solved iteratively for each Newton iteration. The calculation of fluid and geomechanical variables is fully implicit and fully coupled with fluid and heat flow.

MODEL VERTIFICATION

A 1-D column consisting of a double-porosity medium (which may be fissured rock) is considered by Wilson and Aifantis (1982). The conceptual model is shown in Figure 1.

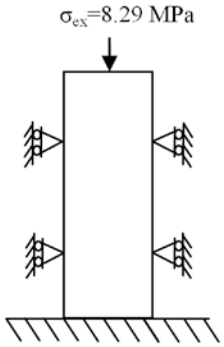

Figure 1. Schematic figure representing a double-porosity model in 1-D fractured reservoirs.

Height of sand column is 50 m. The primary rock properties are basically from Berea sandstone experimental data. The porosity of fracture and matrix is 0.019 and 0.19 respectively. Permeability of fracture and matrix is 1.0×10^{-13} m^2 and 1.0×10^{-17} m^2 respectively. Rock compressibility is 4.40×10^{-10} Pa^{-1}, Poisson ratio is 0.20, Young modulus is 14.40 GPa, and Biot coefficient is 1.0. This actual physical situation occurs in a geothermal reservoir where the initial condition is drained, with zero deformation. When fluid is produced from the reservoir, the rock frame starts to deform. Thus, in our simulation setup, the difference between initial pressure and bottomhole pressure was constructed to be equivalent to pressure change resulting from the top load. Also, the productivity index of the producer is calculated to be equivalent to a constant pressure boundary at the top of reservoir. Analytical and numerical solutions for pressure in fractured media and displacement are shown in Figure 2 and 3. The match is good, adding to the creditability of the model.

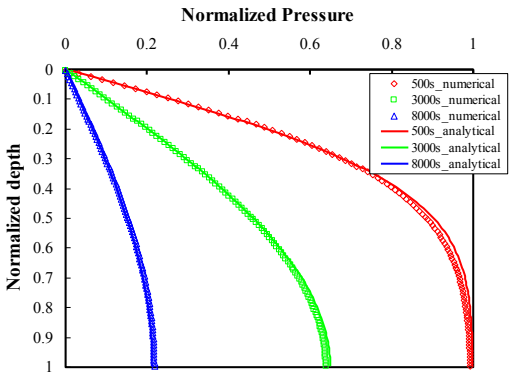

Figure 2. Comparisons of numerical and analytical solutions for pressure in the fracture.

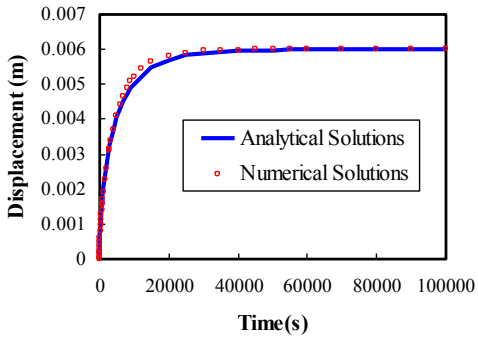

Figure 3. Comparisons of numerical and analytical solutions for normalized displacement at the top of the column.

MODEL APPLICATION

Problem of five-spot injection and production pattern

In geothermal reservoir development, production and injection wells are often sited in regular geometric patterns. In our application, we consider a large well field with wells arranged in a "5-spot" pattern. Because of symmetry, only a quarter of the basic pattern needs to be modeled. Figure 4 shows a simulation in which the fine grids are used near the injection and production wells, whereas coarse grids are used elsewhere. The system is initialized as a normal pressure regime in which subsurface pressure follows the hydrostatic pressure of the water head, and the temperature gradient is set at 4˚C/km. The reservoir is fully saturated with water. Some rock properties are shown in Figure 4.

In this simulation, to analyze the effect of fracturing on pressure and strain distribution, we calculate two scenarios: with and without the consideration of fractures. Figure 5 shows simulation results with consideration of fracturing after 3 years of production near the injector and producers, respectively. Around the injector, the temperature is reduced, as a result of cooling effects, in turn resulting in stress reduction, as can be seen in the pressure and mean normal stress changes following the temperature change pattern (Figure 5(a) and (c)).

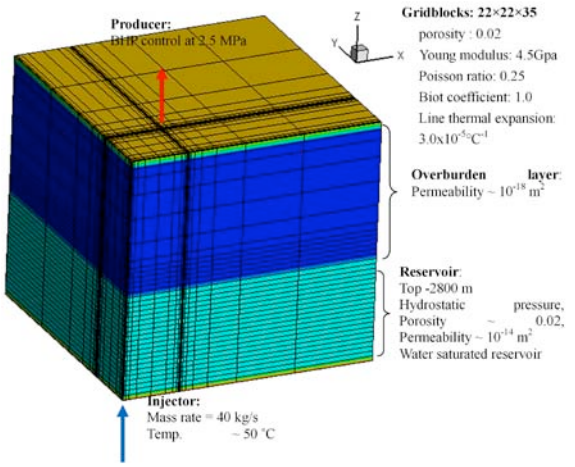

Figure 4. Schematic figure of a quarter model for 5-spot pattern

As shown in Figure 6, the pressure at the injection point in the with-fracture scenario decreases more rapidly than that in the without-fracture scenario; also, volumetric strain is much larger in the with-fracture scenario than in the without-fracture scenario. From Figure 6, the pressure for the with-fracture scenario after 3 years is ~36 MPa, whereas the without-fracture scenario is ~25 MPa. From Figure 7, the total settlement for the with-fault scenario after 3 years is almost 1.50 m, whereas the settlement for the without-fault scenario is less than 0.25 m. The differences in the total settlements demonstrate that the existence of fractures will cause a sharp decline in pressure and large deformation.

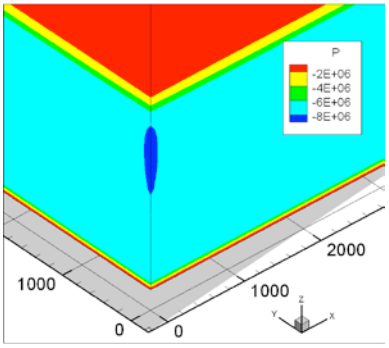

(a) pressure change.

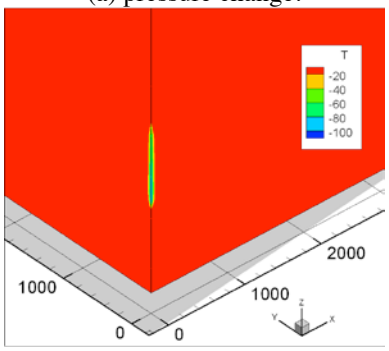

(b) temperature change.

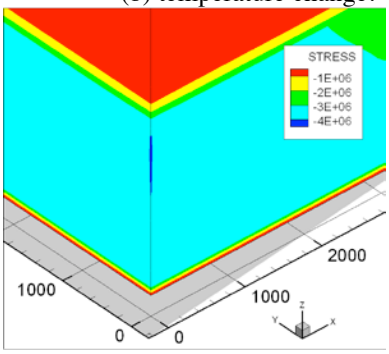

(c) mean normal stress change.

Figure 5. Simulation results with the consideration of fracture at the injector after 3 years.

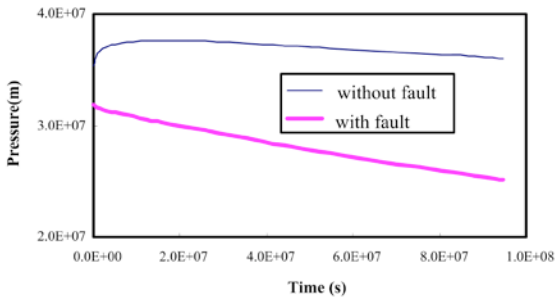

Figure 6. Changes of pressure with time at the injection point

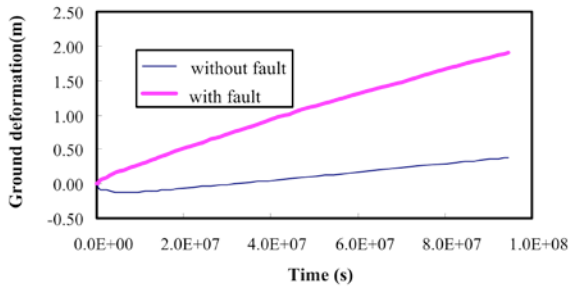

Figure 7. Changes of the total settlement with time at the injection point

The Rutqvist and Tsang CO2 injection model simulation

Rutqvist and Tsang (2002) presented a two-dimensional vertical section model (Figure 8), extended far enough in lateral directions to be considered infinite acting. The injection formation is 200 m thick and bounded by a low permeability basement rock and a 100 m thick cap rock, which in turn is overlain by an upper 1,200 m homogenous formation. The parameters for each formation can be found in Rutqvist and Tsang (2002). Unlike Rutqvist and Tsang (2002) we simulate water injection rather than supercritical CO_2 and focus our study on the effects of the fault. This conducted by comparing the simulation results with and without including the fault into the model simulation.

The functions for porosity and permeability changes are obtained by correlation with laboratory measurements on sandstone (Rutqvist and Tsang, 2002). The porosity, ϕ, is related to the mean effective stress as

$$\phi = (\phi_0 - \phi_r)e^{5\times10^{-8}\cdot\sigma'} + \phi_r \qquad (13)$$

where ϕ_0 is porosity at zero stress, ϕ_r is residual porosity at high stress. Moreover, the permeability is correlated to the porosity according to the following exponential function:

$$k = k_0 e^{22\times(\phi/\phi_r - 1)} \qquad (14)$$

where k_0 is the zero stress permeability.

The simulated pressure, permeability, mean total stress, and volumetric strain profile in the vertical direction for the with-fault scenario after 10 years is shown in Figure 9. Figure 10 shows a comparison of the contour lines of volumetric strain by our model with and without considering faults. In the without-fault scenario, the strain propagates mainly along the bottom of the cap rock, but cannot break through the cap rock. However, in the with-fault scenario, pressure-induced changed in permeability, mean total stress and volumetric strain reach their maximum value around the injection point, and then propagate to the surrounding, and more importantly, changes are found along both the bottom of the cap rock and the fault (Figure 9). When compared with Rutqvist and Tsang's results, the results seem similar and reasonable.

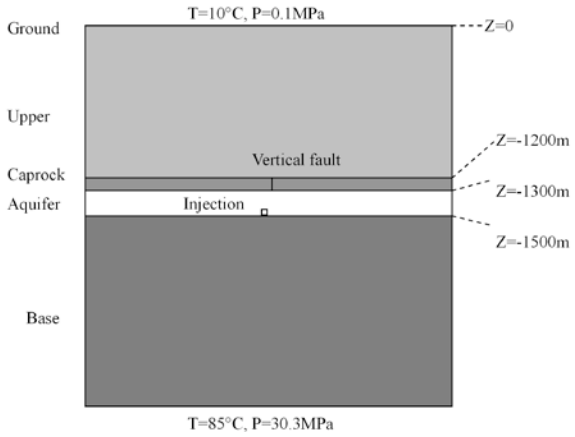

Figure 8. Vertical profile of study area.

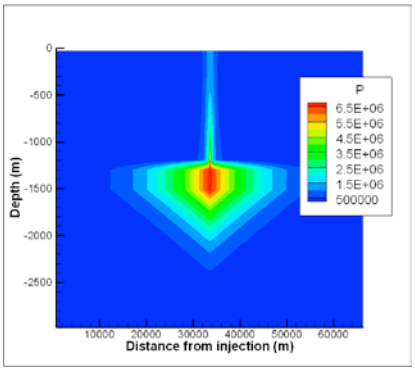

(a) pressure change.

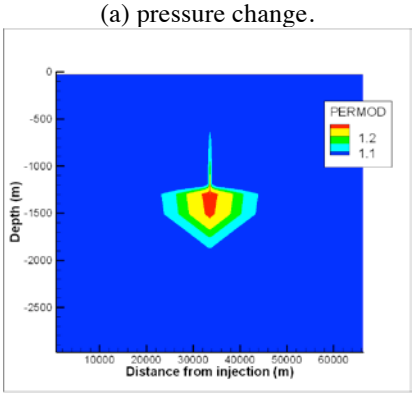

(b) permeability change (K/K_0).

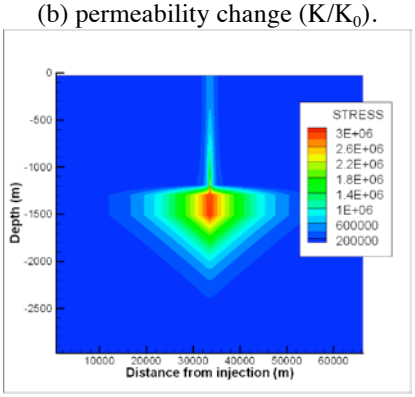

(c) mean normal stress change.

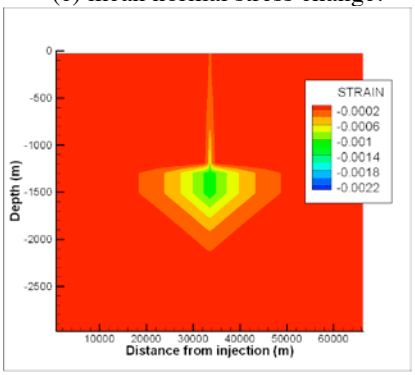

(d) volumetric strain change.

Figure 9. Simulated profile at with-fault scenario after 10 years.

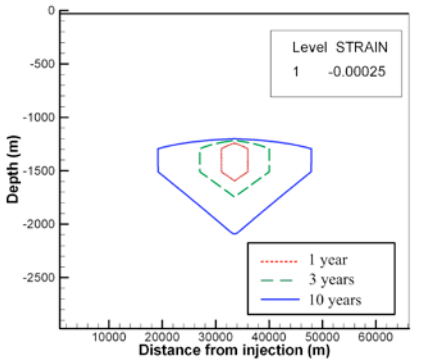

(a) without fault

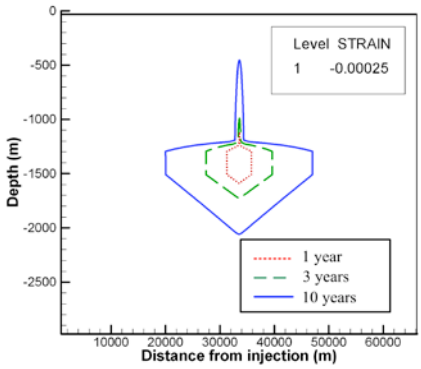

(b) with fault

Figure 10. Simulated contour lines at a value of 0.00025 with-fault and no-fault scenario for 1, 3 and 10 years.

CONCLUSION

We present an efficient, fully coupled fluid flow and geomechanics simulator (TOUGH2-EGS) for simulating multiphase flow, heat transfer, and rock deformation in porous and fractured media. The fluid and heat flow formulation is based on that for TOUGH2/EOS3; the geomechanics formulation is based on the theory of thermo-poroelasticity (the Navier thermo-poroelastic equation). The flow, heat, and stress equations are solved at each Newton-Rapson iteration. The mean total stress is added as an additional primary variable.

Our numerical model is verified for a 1D flow-geomechanics case using a dual porosity method in a fractured reservoir, and is tested by comparison with analytical solutions. In comparing our simulated changes in pressure and strain to analytical model results, we find that our numerical model can produce essentially the same results as analytical models. Two cases—a 5-spot EGS model, and a similar case as posed by Rutqvist and Tsang (2002), are simulated. The results demonstrate that our model can assess how cold water injection and steam or hot water production might affect the stress field in fractured reservoirs—and most importantly, how faults could lead to changes in pressure, stress, and strain.

The presented numerical model only calculates the mean total stress, as opposed to the total stress tensor. Such a simplification may be a shortcoming in our model, since it therefore cannot analyze phenomena dependent on shear stresses, such as rock failure. Also, the model represents instantaneous, undrained responses as well deliverability and changes in the mean normal stress. However, TOUGH2-EGS is rigorous in handling coupled flow and rock deformation and is easily applied to stress-sensible reservoirs for analyzing multiphase fluid, heat flow, and rock deformation in porous and fractured media.

SYMBOLS

Nomenclature

C_R heat conductivity, $W\ K^{-1}\ m^{-1}$.

$\overline{F}$ body force (gravity), Pa m^{-1}.

F^κ the mass or energy transport terms along the borehole due to advective processes, W m^{-1}.

g Gravitational acceleration constant, m s^{-2}.

G shear modulus, Pa.

$h_{\beta w}$ Specific enthalpy in phase βw, J kg^{-1}.

k Absolute permeability, m^2.

K Bulk modulus, Pa.

K_i Bulk modulus, Pa, (i=f, fracture; i=m, matrix)

$k_{r\beta w}$ Relative permeability to phase $\beta\omega$.

M^κ the accumulation terms of the components and energy κ, kg m^{-3}.

$\boldsymbol{n}$ Normal vector on surface element, demensionless.

N the nubers of MINC.

t Time, s.

T Temperature, ˚C or K.

T_i Temperature, ˚C or K, (i=f, fracture; i=m, matrix)

T_{ref} Reference temperature, ˚C or K.

$u_{\beta w}$ the Darcy velocity in phase $\beta\omega$, m s^{-1}.

$U_{\beta w}$ the internal energy of phase β per unit mass, J kg^{-1}

V_b Bulk volume, m^3.

V_n Volume of the n^{th} grid cell, m^3.

P Pressure. Pa.

P_i Pressure of frature. Pa, (i=f, fracture; i=m, matrix)

P_{c0} Reference capillary pressure. Pa.

$P_{\beta w}$ the fluid pressure in phase $\beta\omega$, Pa.

q^{κ} Source/sink terms for mass or energy components, kg $m^{-3}s^{-1}$.

$S_{\beta w}$ Saturation of phase $\beta\omega$, dimensionless.

T Temperature, °C.

$\bar{u}$ Displacement vector, m.

$X^{\kappa}_{\beta w}$ Mass fraction of component κ in fluid phase $\beta\omega$, dimensionless.

Greek Letters

α Biot's coefficient, dimensionless.

α_i Biot's coefficient of fracture, dimensionless, (i=f, fracture; i=m, matrix)

β Linear thermal expansion coefficient, $°C^{-1}$.

β_i Linear thermal expansion coefficient, $°C^{-1}$, (i=f, fracture; i=m, matrix)

β_w fluid phases (=liquid, gas)

$\mu_{\beta w}$ Viscosity, Pa.s

ϕ Porosity, dimensionless.

λ_T Thermal conductivity, $W K^{-1} m^{-1}$

λ Lame's constant, Pa.

ε_{ll} Strain components, l=x,y,z, dimensionless.

ε_v Volumetric strain, dimensionless

$\bar{\bar{\varepsilon}}$ Strain tensor, dimensionless.

ν Poisson's ratio of rock, dimensionless.

σ' Effective stress, Pa.

σ_{ex} External load per area at the top column, Pa.

ρ_R the density of rock grain. kg m^{-3}.

$\rho_{\beta w}$ the density of phase $\beta\omega$, kg m^{-3}.

Γ_n Area of closed surface, m^2.

τ_{kl} k=l for shear stress; k≠l for normal stress, k=x,y,z, l=x,y,z, Pa.

τ_m Mean total stress, Pa.

Subscripts and Superscripts

κ the index for the components, κ = 1 (water), 2 (air), and 3 (energy).

β_w = G for gas; = L for liquid.

ACKNOWLEDGEMENT

This work is supported by the U.S. Department of Energy under Contract No. DE-EE0002762, "Development of Advanced Thermal-Hydrological-Mechanical-Chemical (THMC) Modeling Capabilities for Enhanced Geothermal Systems". This work is also supported by the CMG Foundation and the National Nature Science Foundation of China (Grant Numbers: 41072178 and 40872159).

REFERENCES

Bai, M., Roegiers, J.-C., Fluid flow and heat flow in deformable fractured porous media, *Int. J. Engng Sci.*, 32(10), 1615-1633, 1994.

Bai, M., Roegiers, J.-C., Elsworth, D., Poromechanical response of fractured-porous rock masses, *J. Petroleum Sci. Engng.*, 13, 155-168, 1995.

Barenblatt GI, Zheltov IP, and Kochina IN. Basic concepts in the theory of seepage of homogeneous liquids in fissured rocks. PMM, Sov Appl Math Mech, 24(5):852-864, 1960..

Boutt, D.F., Cook, B.K., Williams, J.R., A coupled fluid-solid model for problems in geomechanics: application to sand production, *International Journal of Numerical and Analytical methods in Geomechanics*, 35, 997-1018, 2011.

Doughty, C., Investigation of conceptual and numerical approaches for evaluating moisture, gas, chemical, and heat transport in fractured unsaturated rock, *J. Cont. Hydro.*, 38, 69-106, 1999.

Jaeger, J. C., N. G. W. Cook, and R. W. Zimmerman, *Fundamentals of rock mechanics.* Blackwell, Forth edition, 2007.

Lewis, R.W., Schrefler, B.A., *The finite element method in the static and dynamic deformation and consolidation of porous media*. Chichester, England: Wiley, ^{2}nd edition. 1998.

Merle, H.A., Kentie, C.J.P., Van Opstal, G.H.C., Schneider, G.M.G., 1976. The Bachaquero Study-a composite analysis of the behavior of a compaction drive/solution gas drive reservoir. *JPT*, 1107–1114.

Pruess, K., and T.N. Narasimhan, A practical method for modeling fluid and heat flow in fractured porous media, *Soc. Pet. Eng. J.*, 25(1), 14-26, 1985.

Pruess, K., C., Oldenburg, and G., Moridis, *TOUGH2 User's Guide, V2.0*, Lawrence Berkeley National Laboratory Report LBNL-43134, Berkeley, CA, 1999.

Rutqvist, J., Tsang, C.F., A study of caprock hydromechanical changes associated with CO_2-injection into a brine formation, *Environmental Geology*, 42, 296–305, 2002.

Settari, A., Walters, D.A., Advances in coupled geomechanical and reservoir modeling with applications to reservoir compaction, *SPE Journal*, 6(3), 334-342, 2001.

Warren, J.E., and P.J., Root, The behavior of naturally fractured reservoirs, *Soc. Pet. Eng. J.*, 245-255, 1963.

Wilson, R.K., Aifantis, E.C., On the theory of consolidation with double porosity, *Int. J. Engng. Sci.*, 20(9), 1009-1035, 1982.

Winterfeld, P.H., Wu, Y.S., Parallel simulation of CO_2 sequestration with rock deformation in saline aquifers, *Society of Petroleum Engineers*, *SPE 141514*, 2011.

Wu, Y. S., H. H. Liu, and G. S. Bodvarsson, A triple-continuum approach for modeling flow and transport processes in fractured rock, *Journal of Contaminant Hydrology*, 73, 145-179, 2004.